2D Extraction of Open-Circuit Impedances of Three-Phase Transformers

E. A. Gutierrez-Rodriguez[2], R. Escarela-Perez[1,*], J. C. Olivares-Galvan[1], M. S. Esparza-González[2] and E. Campero-Littlewood[1]
[1]Universidad Autonoma Metropolitana - Azcapotzalco, Departamento de Energia, Av. San Pablo 180, Col. Reynosa, C.P. 02200, Mexico D.F., MEXICO, [2]Instituto Tecnologico de Aguscalientes, Av. Adolfo López Mateos 1801 oriente., Aguascalientes, Aguascalientes, MEXICO.
*Corresponding author: Av. Cuauhtemoc 963, Depto 404A, Col. Narvarte Poniente, Mexico, D.F., MEXICO, r.escarela@ieee.org

Abstract: This work is concerned with the study of the asymmetrical phenomenon observed in three-phase transformers during the standard short-circuit test. The purpose of our work is to see if the asymmetric measurements can be predicted with the use of 2D finite-element models. To this end, we use the AC/DC module of COMSOL Multiphysics. A multi-port network impedance is then determined to explain the main source of asymmetry.

Keywords: Distribution transformers, load-loss test, 2D finite element modeling.

1. Introduction

Low-Frequency transformers are widely used in power networks for efficient utilization of electric energy. Its basic functioning has been understood since the end of the nineteen century and taught in electrical engineering courses. However, the basic theory that leads to the classic equivalent circuit of the transformer is unable to describe intriguing behavior observed during certain operating conditions. It is therefore necessary to resort to more advanced tools to determine the electromagnetic fields that truly characterize transformers. The low-frequency transformer can be described in 2D with the diffusion equation in terms of the magnetic vector potential. This way it is possible to model filamentary and massive conductors, as well as magnetic non-linear materials. Interconnection with external systems is also possible using the voltages and current equations of the 2D domain conductors. As a result, any operating condition of the transformer can be simulated.

The load losses in a transformer are commonly measured by a three-wattmeter method. It is generally found that the three readings are appreciably different, even though the total losses (addition of the three readings) are near to the design value. The stray loss may form an appreciable part of the total load loss in power transformers. Hence, the simplest explanation which may normally be given is that the stray loss for each phase could be different due to the asymmetry of tank and other structural parts. However, this explanation is marginally true.

The asymmetry observed during the no-load test has been fully discussed in the literature [1-4]. This magnetizing asymmetry, which results in different currents and powers of the three phases, occurs due to asymmetry in magnetic reluctances offered to the three phase fluxes. On the other, the load-loss test represents a more complicated problem since all phases are interacting and the loss and magnetic field distribution show more complex patterns.

An interesting work [5] that sheds light on asymmetry during the load-loss test has been presented until very recently. Magnetic circuit theory is used there to explain the asymmetry phenomenon. However, the numerical model is not rigorously deduced from transformer geometry and material properties. The finite-element method has been recently used [6] to explain the asymmetry phenomenon using a time-harmonic and three-dimensional model. It was found that the main causes of asymmetry are the unequal magnetic coupling between phases. Ref [7] has extended this work to mathematically prove that asymmetry will always exist in distribution transformers with cores of standard geometry.

3D finite-element modeling requires extensive computational resources and geometry modeling may become cumbersome. So, it becomes desirable to assess the possibility of using 2D finite-element modeling to study the asymmetry in transformers despite the fact of having true 3D geometries. This way, this work addresses this question using the AC/DC module of COMSOL and determining a multi-port impedance network.

2. Magnetic Field Equations

Maxwell's equations that fully describe the modeling of low-frequency electromagnetic devices in two dimensions are:

$$\begin{aligned} \nabla \times E &= -\frac{\partial B}{\partial t} \\ \nabla \cdot B &= 0 \\ \nabla \times H &= J \end{aligned} \tag{1}$$

where the displacement current and free charges have been disregarded. *E*, *B*, *H* are the electric field, the magnetic flux density and the magnetic field, respectively. They are strictly contained in a plane. *J* is the current density and its direction is perpendicular to the plane of *E*, *B* and *H*. Equations (1) can be combined to give for 2D problems the following diffusion-type equation:

$$\sigma \frac{\partial A}{\partial t} + \nabla \times \left(\frac{1}{\mu_0 \mu_r} \nabla \times A\right) = \frac{\sigma \Delta V}{d} + J^e \tag{2}$$

with $B = \nabla \times A$, where *A* is the magnetic vector potential and is parallel to *J*, μ_0 is the magnetic permeability of vacuum and μ_r is the relative permeability. J^e is an external current density imposed in conductor regions and it is also parallel to *J*. It is uniform at the conductor cross section. Conductors have length *d* with a potential difference ΔV which is usually unknown. Analytical solution of (2) is difficult or impossible for electrical machines due to their intricate geometries, proper consideration of material properties and external elements interacting with them.

2.1 Time-harmonic representation

If all magnetic and electric quantities have sinusoidal variation with an electrical angular speed ω, they can be conveniently represented in the frequency domain using the classical phasor concept of circuit theory. This way, *E*, *B*, *H* and J^e, ΔV are now complex quantities whereas $\partial/\partial t$ is substituted by $j\omega$. Equation (2) can then be rewritten as:

$$j\omega\sigma A + \nabla \times \left(\frac{1}{\mu_0 \mu_r} \nabla \times A\right) = \frac{\sigma \Delta V}{d} + J^e \tag{3}$$

3. Multi-port impedance network

Three-phase transformer self and mutual impedances can be defined in terms of a six-port network, each port corresponding to each of the six transformer windings (3 low-voltage (LV) and 3 high-voltage (HV) windings). This way, a set of 36 impedances are required to fully define the electromagnetic behavior of the transformer. Thus, a multi-port network [8] can be written in terms of the so called open-circuit impedances as follows:

$$\begin{Bmatrix} V_A \\ V_B \\ V_C \\ V_a \\ V_b \\ V_c \end{Bmatrix} = \begin{bmatrix} Z_{AA} & Z_{BA} & Z_{CA} & Z_{aA} & Z_{bA} & Z_{cA} \\ Z_{AB} & Z_{BB} & Z_{CB} & Z_{aB} & Z_{bB} & Z_{cB} \\ Z_{AC} & Z_{BC} & Z_{CC} & Z_{aC} & Z_{bC} & Z_{cC} \\ Z_{Aa} & Z_{Ba} & Z_{Ca} & Z_{aa} & Z_{ba} & Z_{ca} \\ Z_{Ab} & Z_{Bb} & Z_{Cb} & Z_{ab} & Z_{bb} & Z_{cb} \\ Z_{Ac} & Z_{Bc} & Z_{Cc} & Z_{ac} & Z_{bc} & Z_{cc} \end{bmatrix} \begin{Bmatrix} I_A \\ I_B \\ I_C \\ I_a \\ I_b \\ I_c \end{Bmatrix} \tag{4}$$

where uppercase letters refer to the HV side, while lowercase letters refer to the LV side. Winding currents and voltages are explicitly written in phasor form. The name of open-circuit impedances arises from (4), which shows that mutual impedances can be calculated individually as:

$$Z_{ij} = \left.\frac{V_i}{I_j}\right|_{I_k = 0, \forall_{k \neq j}} \tag{5}$$

This equation simply states that a mutual impedance, between port windings *i* and *j*, can be obtained by measuring the open-circuit voltage on port *i*, that is caused by the current entering port *j*. It is understood that all other ports are open and do not carry currents. The self impedances are also obtained by making *j*=*i*.

4. 2D Finite-Element Extraction of Transformer Impedances

A three-phase, 31.5MVA, 132kV/33kV, star-delta transformer is considered in this work. The transformer is designed to connect its HV windings in star, while its LV windings are connected in delta. Each of the LV and HV windings has 433 and 1000 turns, respectively. Windings are concentrically wound around the core limbs. Figure 1 shows the main dimensions of this transformer.

The AC/DC module of COMSOL has been used to simulate the time-harmonic operation of the transformer. This module can handle the following 2D partial differential equation:

$$\begin{aligned}(j\omega\sigma - \omega^2\varepsilon_0\varepsilon_r)A + \nabla\times(\mu_0^{-1}\mu_r^{-1}\nabla\times A)\\ - \sigma \mathrm{v}\times(\nabla\times A) = \frac{\sigma\Delta V}{d} + J^e\end{aligned} \qquad (6)$$

where ε_r and ε_0 are the relative and vacuum permittivities, respectively. v is a velocity term that may account for moving conductors in problems where the same geometry is preserved as the conductor changes position. If ε_r and v are set to zero, it is readily seen that equation (3) is obtained and COMSOL can deal with the transformer modeling problem of this work.

Six simulations were performed to obtain the 36 impedances of (4). They involve the individual injection of current into each of the six phases according to (5). Since a constant permeability of the transformer core is assumed, the simulation problem is rendered linear and an arbitrary current value will lead to the same impedance value (when dividing the induced voltages by this current). So, an injection of one ampere has been chosen here to make the induced voltage values equal to the impedance ones (as can be seen from (5).

The only solid conductor present in the transformer is the tank which is assumed earthed and, therefore, the ΔV term in (6) is set to zero. The eddy current effect is modeled with the $j\omega\sigma A$ term. The skin depth must be considered during the construction of the finite-element mesh. The size of the elements in the solid conductor region should be close to the skin depth to properly model the eddy currents. Figure 2 shows the finite element mesh obtained with COMSOL's automatic mesh generator. It can be seen that a lot of elements have been placed in the tank region.

Boundary conditions have been set up as follows. A Dirichlet boundary condition has been assigned to the outer surface of the tank. This can be easily justified since the penetration of eddy currents is smaller than the tank thickness and the magnetic flux cannot reach the outer tank surface. Symmetry of excitations and geometry allow the use of a Neumman boundary condition to only model one half of the full geometry.

The transformer impedances are obtained once the finite-element results provided by COMSOL are available. The procedure is as follows. The general expression of the magnetic flux is given by [8]:

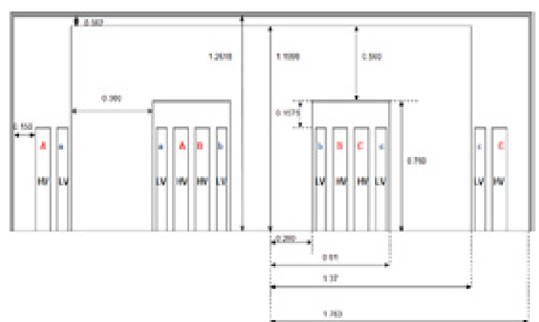

Figure 1. Main dimensions of the transformer geometry. Units in meters.

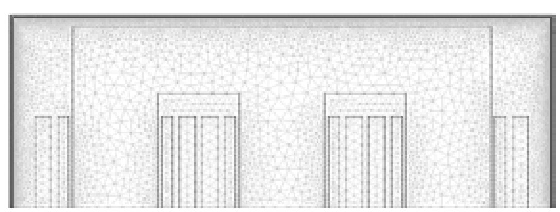

Figure 2. Finite Element Mesh created with COMSOL's automatic mesh generator.

$$\phi = \oint \vec{A}\cdot d\vec{l} \qquad (7)$$

where the "hat" arrows indicate vector quantities. Equation (7) is greatly simplified for 2D problems governed by (3), since the magnetic vector potential has only one component. As a result, the magnetic flux that passes through two points can be calculated as:

$$\phi = (A_2 - A_1)d \tag{8}$$

where A_2 and A_1 are the potential values at the two points. This expression cannot be directly applied to calculate the magnetic flux that crosses the transformer windings since they are not concentrated in one single point. They are occupying a finite surface S and a single magnetic vector potential cannot be defined. However, equation (8) can still be used if an average value of the magnetic vector potential in the surface S is calculated as:

$$\overline{A} = \frac{1}{S}\iint_s A d\Omega \tag{9}$$

where $\overline{A}$ is the average value of A. Hence, the flux linkages of any of the transformer windings can be written as:

$$\lambda = N(\overline{A}_{go} - \overline{A}_{return})d \tag{10}$$

$\overline{A}_{go}$ is the average potential on the winding turns that go into the 2D model while $\overline{A}_{return}$ is the average potential of the winding turns that come out. N is the number of winding turns. Notice that the go and return turns form one winding. As a result, there are 12 surfaces modeling the six phases of the transformer. The voltage equation of any winding is then given in the frequency domain by:

$$v = ir + j\omega\lambda \tag{11}$$

where r is the total resistance of the winding conductors. Equations (11) can be readily computed using COMSOL's integration coupling variables at appropriate subdomains.

5. Numerical Results

Figures 3 to 5 show the calculated magnetic flux distributions at ωt = 0° when the LV windings are excited. The flux distributions for the HV windings are omitted since they are "visually" identical to their corresponding LV windings. The asymmetry of magnetic flux is immediately seen in Figures 3 and 5, where the main flux is unequally distributed in the remaining two core legs. This visual fact is reflected in unequal magnetic couplings.

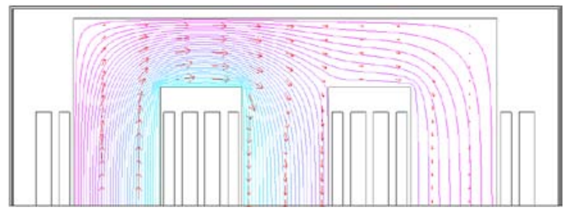

Figure 3. Magnetic flux distribution at ωt = 0°. Phase *a* excited.

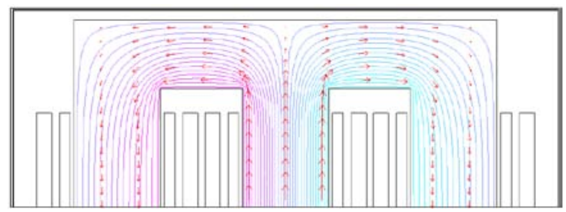

Figure 4. Magnetic flux distribution at ωt = 0°. Phase *b* excited.

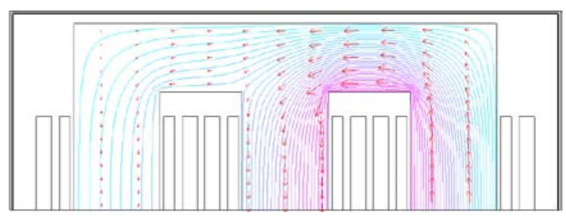

Figure 5. Magnetic flux distribution at ωt = 0°. Phase *c* excited.

Tables 1 and 2 summarize the open-circuit calculations. They give the open-circuit induced voltages at winding terminals when each winding in turn is fed with one ampere. For instance, the first row of Tables 1 and 2 gives the values (in volts) of the induced voltages for the case of winding A. The particular value of a induced phase voltage due to a particular phase current is obtained from the tables by the letters that identify the HV and LV windings (e.g., the induced voltage of C due to current in A is located in the first row and third column of table 1). Moreover, the two tables can be seen as impedance matrices that constitute the impedance matrix in (4).

Table 1: Induced Voltages from Open-Circuit Tests: Part I

	A	B	C
A	-96.49-*j*2.16e6	-13.19+*j*1.56e6	1.05+*j*5.97e5
B	-13.19+*j*1.56e6	-27.69-*j*3.12e6	-13.19+*j*1.56e6
C	1.05+*j*5.97e5	-13.19+*j*1.56e6	-96.48-*j*2.15e6
a	-39.99-*j*9.34e5	-5.50+*j*6.75e5	0.53+*j*2.58e5
b	-5.71+*j*6.75e5	-11.55-*j*1.35e6	-5.71+*j*6.75e5
c	0.53+*j*2.59e5	-5.50+*j*6.75e5	-39.99-*j*9.34e5

Table 2: Induced Voltages from Open-Circuit Tests: Part II

	a	b	c
A	-39.99-*j*9.34e5	-5.71+j6.75e5	0.53+*j*2.58e5
B	-5.50+*j*6.75e5	-11.55-*j*1.35e6	-5.50+*j*6.75e5
C	0.53+*j*2.58e5	-5.71+*j*6.75e5	-39.99-*j*9.34e5
a	-16.93-*j*4.04e5i	-2.38+*j*2.92e5	0.26+*j*1.12e5
b	-2.38+*j*2.92e5	-5.13-*j*5.85e5	-2.38+*j*2.92e5
c	0.26+*j*1.12e5	-2.38+*j*2.92e5	-16.92-*j*4.04e5

The following facts can be observed from the two tables. The impedance system complies with the reciprocity theorem of passive linear networks, that is, $Z_{ij}=Z_{ji}$. The real parts of the self impedances account for winding and stray losses, whereas the real parts of the mutual impedances only take into consideration the stray losses. The impedance asymmetries produce different power readings and current unbalance when the load-loss test is performed.

Tables 1 and 2 have been compared with their corresponding ones in [7]. It was found that the asymmetry is correctly predicted in both 3D and 2D representation. However the impedance values show very large deviations. This means that a 2D approximation cannot be used to approximate the true 3D nature of the transformer.

Now, it is possible to use the multi-port network to compute the short-circuit currents of the load-loss tests as follows. The network model can be used to obtain the winding currents produced by applying a short-circuit at the low-voltage terminals, whereas the high-voltage windings are fed with impedance voltages, this way representing the load-loss test. Equation (4) can be simply written as {V}=[Z]{I}, such that:

$$\{I\}=[Y]\{V\} \qquad (12)$$

The element entries of [Y] are called the short-circuit admittance parameters of the passive network. The specification of $\{V\}^T = \{10921 \angle 0° \;\; 10921 \angle -120° \;\; 10921 \angle 120° \;\; 0 \;\; 0 \;\; 0\}$ in (12) gives the short-circuit condition that represents the load-loss test. The value of 10921 corresponds to impedance voltage. High-voltage input powers are found from the following phasor operations: $P_i = Re(V_i I_i^*)\big|_{i=A,B,C}$. Table 3 summarizes the results obtained from the six-port network model. These results have also been compared with those provided in [7]. It was found again that the 2D model is unable to provide accurate numerical results.

Table 3: Calculated Currents and Powers from Six-Port Network Model.

Limb	HV Current [A]	LV Current [A]	Input Power
right	33.14∠90.48°	77.04∠-90.09°	-3067.6
middle	33.36∠-150.25°	76.14∠29.72°	1589.4
left	33.07∠-31.25°	76.80∠149.36°	7855.7

6. Conclusions

A 2D finite-element analysis has been performed to study the asymmetry phenomenon of three-phase distribution transformers observed during the load loss-test. The impedances of a multi-port network have been determined to show that asymmetry is mainly produced by unequal magnetic couplings. It has been found that a 2D representation is able to predict this behavior but a 3D representation is unavoidable if accurate numerical results are required for quantities measured at the terminals of ports. The authors are currently investigating correcting factors to increase the accuracy of the 2D numerical model.

7. References

1. J. I. Parion, Magnetizing unsymmetry in three-phase core-type transformers, *Elect. Energy*, pp. 330–336, Jul. 1957.

2. C. S. Walker, The excitation requirement of 3-phase core-type, 3-legged y-connected transformer, *AIEE Trans.*, pp. 1113–1119, Dec.1957.
3. A. S. Nene, S. V. Kulkarni, and K. Vijayan, Asymmetrical magnetizing phenomenon of three-phase core-type transformers, *in Proc. Int. Conf. Transformers, TRAFOTECH*, vol. 15, pp. IV 21–26, Jan. 1994.
4. S. V. Kulkarni and S. A. Khaparde, Transformer Engineering: Design and Practice. New York: Marcel Dekker, May 2004.
5. P. Picher, L. Bolduc, R. Gagnon, and G. Sybille, Study of the apparent load loss unbalance in three-phase transformers, *in Proc. 18th Annu.Can. Conf. Electrical and Computer Engineering, CCECE/CCGEI*, Saskatoon, SK, Canada, pp. 1473–1476, May 2005.
6. R. Escarela-Perez, S. V. Kulkarni, N. K. Kodela and J.C. Olivares-Galvan, Asymmetry during load-loss measurement of three-phase three-limb transformers, *IEEE Transactions on Power Delivery*, **Vol. 22**, No. 3, pp. 1566-1574, 2007.
7. R. Escarela-Perez, S. V. Kulkarni, J. Alvarez-Ramirez and K. Kaushik, Analytical Description of the Load-Loss Asymmetry Phenomenon in Three-Phase Three-Limb Transformers, *IEEE Transactions on Power Delivery*, **Vol. 24**, No. 2, pp. 695-702, 2009.
8. W. H. Hayt and J. E. Kemmerly, Engineering Circuit Analysis, 5th ed. New York: McGraw-Hill, 1996.

9. Acknowledgements

This work was supported in part by the National Council of Science and Technology (CONACYT-MEXICO) and in part by the National System of Researchers (SNI-MEXICO).